

NEW TEMPERATURE CONSTRAINTS OF MERCURY'S VOLATILE POLAR DEPOSITS. Colin D. Hamill¹, Nancy L. Chabot¹, Erwan Mazarico², Matthew A. Siegler³, and Michael K. Barker², ¹Johns Hopkins University Applied Physics Laboratory, Laurel, MD 20723, USA (Colin.Hamill@jhuapl.edu). ²NASA Goddard Space Flight Center, 8800 Greenbelt Rd., Greenbelt, MD 20771, USA. ³Planetary Science Institute, 1700 E Fort Lowell Rd, Tucson, AZ 85719, USA.

Introduction: Earth-based radar observations and multiple datasets from the MErcury Surface, Space ENvironment, GEochemistry, and Ranging (MESSENGER) mission have provided evidence that Mercury's polar regions host volatile deposits dominantly composed of water ice [1-7]. However, the majority of the deposits are located in regions that are too warm to support water ice at the surface [3], and low surface reflectance observed in these regions has been interpreted to indicate lag deposits of organic-rich, volatile material [3-5]. The highest resolution images of these polar deposits by MESSENGER's Mercury Dual Imaging System (MDIS) revealed low-reflectance surfaces with sharp boundaries and intriguing brightness variations, and understanding these features can provide key insight into the nature and composition of Mercury's volatile polar deposits, with implications for their age and origin.

However, interpretation of the highest resolution images of Mercury's volatile polar deposits has been limited by the available topography, illumination, and temperature models. Existing models were primarily concerned about Mercury's north polar region as a whole [3, 6]. Fortunately, due to MESSENGER's highly eccentric near-polar orbit, for latitudes near 80-85°N, the density of Mercury Laser Altimeter (MLA) tracks enables higher resolution, local digital elevation models (DEMs) to be made, which themselves enable higher-resolution illumination and thermal models. In this work, we focus on the 25-km-diameter crater Ensor. Ensor is known to have stark brightness variations and sharp boundaries in high-resolution MESSENGER images [8] and is also situated in a region with a high density of MLA tracks, making it an ideal candidate for our high-resolution study of the nature of Mercury's polar volatile deposits.

Methods: High-density MLA tracks along with photoclinometry from MDIS images [10] were used to create a local DEM of Ensor at 125 m/pixel (Fig. 1A), considerably higher than the 500 m/pixel version available for the full north polar region [6]. From this DEM, slope (Fig. 1B) and percent solar illumination (Fig. 1C) were derived, using the methods of [6].

Thermal model calculations were performed with a triangular mesh derived from the DEM, following the methods of [3]. Maps from the thermal model calculations were created at a resolution of 125 m/pixel, much higher than the 1 km/pixel thermal simulation of the full polar region [3]. The models include the maximum surface temperature over a Mercury solar day (Fig. 1D), as well as average subsurface temperature and depth for volatiles (water, sulfur, and coronene).

Using broadband images obtained by the MDIS Wide-Angle Camera (WAC), MESSENGER was able to obtain images of Ensor's permanently shadowed region (PSR) [8]. After examining all WAC broadband images for Ensor, six distinct images were selected for our study that span the available range of emission angles of 0°-34° and phase angles of 66°-118°. These images had resolutions of 38-91 m/pixel.

All Ensor images and datasets were registered to the DEM and mapped to a polar stereographic projection at a resolution of 38 m/pixel (the highest image resolution in the dataset), using the United States Geological Survey's Integrated Software for Imagers and Spectrometers.

Results: Our new high-resolution model results show that the small-scale brightness variations noted previously within Ensor's PSR [8, 9] (Fig. 2A) correlate with the slope variations of the crater's floor and walls (Fig. 2B). This correlation raises the possibility that the brightness variations within the WAC broadband images of Ensor may be due to viewing geometry effects. Further work is needed to confidently distinguish viewing geometry effects due to the complicated scattered light illumination conditions of these WAC broadband images versus variations proposed to be due to volatile composition differences [8] or ejecta from small craters [9].

Comparing the WAC broadband images to the illumination map reveals clearly that the sharp, low-reflectance boundary in the images extends slightly beyond the PSR (Fig. 2C). The low-reflectance boundary aligns well with a very low illumination percentage of 0.01% averaged over a Mercury solar day, indicating that certain low-reflectance volatiles are still

stable on Mercury's surface even when receiving a small amount of direct sunlight.

The low-reflectance boundary corresponds with a maximum temperature of 300-350K (Fig. 2C). This temperature range also corresponds to the point where coronene ($C_{24}H_{12}$) is no longer stable on the surface (Fig. 2D). While coronene is a striking match to the low-reflectance boundary in Fig. 2D, coronene should be viewed as representative of complex organic compounds with molecular masses similar to ~ 300 g/mol rather than a specific identification of the low-reflectance material in Ensor.

Overall, the temperature models support the idea that complex organic volatile compounds reside within Ensor's PSR and are responsible for the low-reflectance surface. Our results provide new evidence that indicates that the low-reflectance surface extends beyond the strictly PSR and into dimly lit regions of the crater, consistent with the modeled stability of complex

organic compounds. Our future work will be focused on analyzing other craters at similar latitudes and with similar high-resolution models to evaluate if these results from Ensor are consistent between Mercury's volatile polar deposits.

References: [1] Harmon J.K. et al. (2011) *Icarus*, 211, 37–50. [2] Lawrence D.J. et al. (2013) *Science*, 339, 292–296. [3] Paige D.A. et al. (2013) *Science*, 339, 300–303. [4] Neumann G.A. et al. (2013) *Science*, 339, 296–300. [5] Chabot N.L. et al. (2014) *Geology*, 42, 1051–1054. [6] Deutsch A.N. et al. (2016) *Icarus*, 280, 158–171. [7] Chabot N.L. et al. (2018) 346–370. [8] Chabot N.L. et al. (2016) *GeoPhys Res. Lett.*, 43, 9461–9468. [9] Deutsch A.N. et al. (2019) *EPSL*, 520, 26–33. [10] Beyer R.A. et al. (2018) *ESS*, 5, 537–548.

Acknowledgements: NASA DDAP grant 80NSSC19K0881, NASA PSD Research Program.

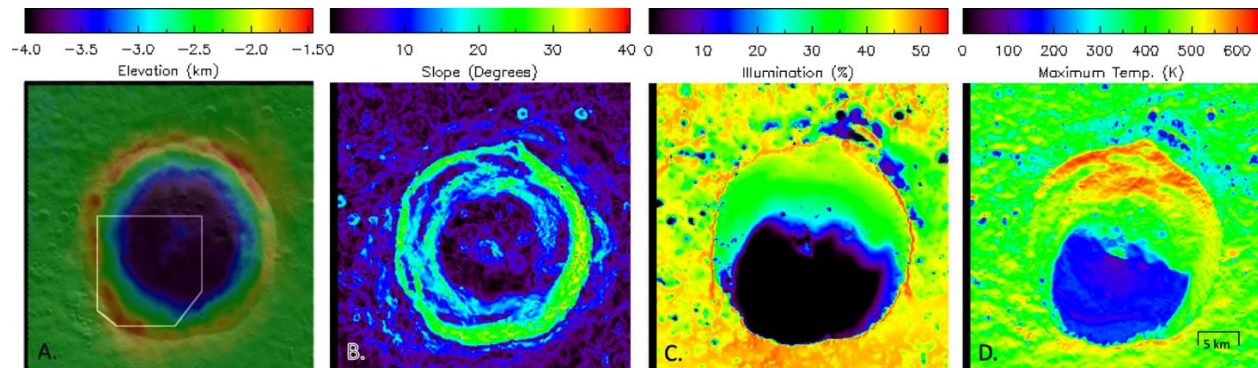


Figure 1. High-resolution models of Ensor (25 km diameter): **A.** DEM, overlain on image mosaic and outline of image EW1051458815B. **B.** Slope. **C.** Average percent illumination over a Mercury solar day **D.** Maximum surface temperature throughout a Mercury solar day.

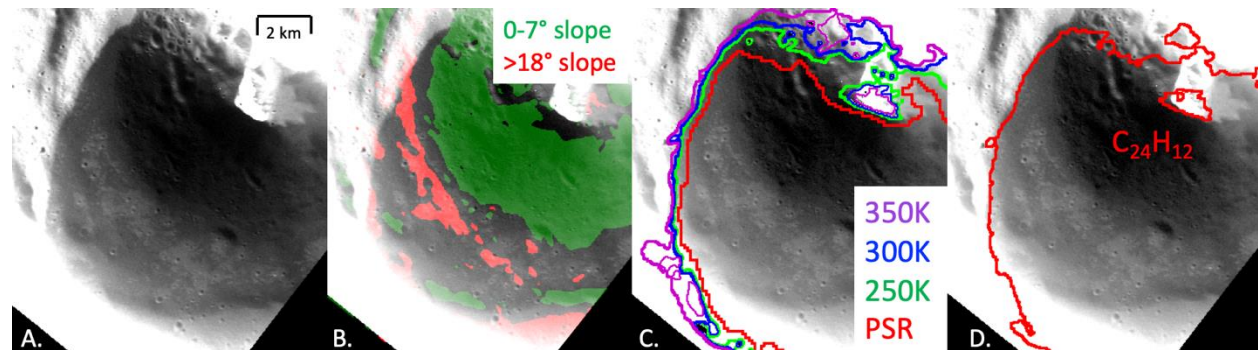


Figure 2. **A.** WAC broadband image EW1051458815B (38 m/pixel) of Ensor's low-reflectance surface within the permanently shadowed region. **B.** Shading of low slope ($0-7^\circ$, green) and high slope ($>18^\circ$, red) regions. **C.** Outline of permanently shadowed region (red) and 250K, 300K, 350K temperature boundaries (green, blue, purple). **D.** Outline of region where coronene ($C_{24}H_{12}$) is thermally stable on the surface.